LETTER

Small fish eat smaller fish: A model of interaction strength in early life stages of two tuna species

Daniel Ottmann [ID],[1]* Patricia Reglero,[1] Francisco Alemany,[1] Diego Alvarez-Berastegui,[1] Melissa Martín,[1] Øyvind Fiksen[2]
[1]Centro Oceanográfico de Balears (IEO, CSIC), Palma de Mallorca, Spain; [2]Department of Biological Sciences, University of Bergen, Bergen, Norway

Scientific Significance Statement

Most marine fishes die during their first days of life falling prey for other animals, and even minor changes in early predation rates can lead to order-of-magnitude variation in the number of individuals recruiting to the adult population. However, quantifying predation in fish early life stages and linking species-specific interactions to recruitment and population dynamics is challenging. Here, we test the hypothesis that recovery of the commercially exploited Atlantic bluefin tuna can affect early survival of the Mediterranean albacore through predator–prey interactions of their early life stages. We find that when the predator species is present, they have a large predatory capacity on the prey species, but their patchy distribution may limit their total effect. Along with other processes affecting early survival, this interaction can contribute to a loss of recruitment potential to later stages.

Abstract

Fish larvae are rarely a major driver of fish mortality, but tunas can produce large batches of larvae that rapidly develop the capacity to kill other fish. We combine a model for the killing potential from Atlantic bluefin tuna (BFT) larvae on larval albacore (ALB) with field observations at a major spawning ground. Both species spawn from June to August, but BFT has a narrow spawning peak at the beginning of the season that results in priority effects. Our model shows that, following a recent stock recovery, BFT larvae have increased their killing pressure, leaving areas of up to 1000 km^2 with < 1% chance of ALB daily survival. Such increase in killing pressure suggests larval ALB has reduced chances to survive; yet in large areas with few BFT, other drivers of early survival prevail over BFT predation. This shows that strong predatory interactions can occur during larval stages in some fishes.

*Correspondence: daniel.ottmann.riera@gmail.com

Can predation by days-old fish larvae change reproductive success in other fish species? Although most fishes get killed by predators early in their life, piscivorous fish larvae are usually considered a minor cause of mortality because they are a small fraction of the total predator guild (Bailey and Houde [1989](#); Folkvord [1997](#); Houde [2008](#)). This paradigm is likely true for most fishes, but some highly piscivorous fishes like tunas rapidly develop morphological traits (fast swimming speed, large eyes, large mouth-gap, voracious behavior, and rapid development of digestive system) that turn them into effective piscivores (Kaji et al. [2002](#); Llopiz and Hobday [2015](#)). Furthermore, adults are highly fecund fishes that target spawning grounds shared with other tunas, facilitating encounters among larvae (Reglero et al. [2014](#)). The Mediterranean albacore *Thunnus alalunga* (hereafter ALB) and Atlantic bluefin tuna (BFT) *Thunnus thynnus* are large, migratory species that share a major spawning ground in the western Mediterranean Sea (Alemany et al. [2010](#)). Here, they spawn from June to August, but BFT has a narrower spawning peak than ALB, shifted toward the beginning of the breeding season (Saber et al. [2015](#); Reglero et al. [2018b](#)).

During the tuna spawning season in the Mediterranean Sea, invertebrate predators are few and patchy (Ottmann et al. [2021](#)), but piscivorous fish larvae may be important predators of smaller larvae. The fact that BFT and ALB can produce large batches of larvae that are restricted to the warm water above the shallow (~ 20 m depth) thermocline (Torres et al. [2011](#); Reglero et al. [2018a](#)) increase encounter rates and strengthen interactions. However, the strength of predatory interactions among tuna larvae has never been quantified.

Can predation from BFT larvae limit the early survival of ALB? The current rise of the eastern stock of Atlantic BFT (ICCAT [2020](#)) and the concurrent decline of ALB makes this question relevant and provides an opportunity to explore this interaction. After decision makers implemented strict fishing quotas on BFT, the eastern stock has boosted from 348 thousand MT in 2007 to over 1 million MT in 2018 (Porch et al. [2019](#); ICCAT [2020](#)). In contrast, the unmanaged population of Mediterranean ALB has recently declined in different parts of the sea (Alvarez-Berastegui et al. [2018](#); ICCAT [2021](#)). This decline cannot be attributed to fisheries because fishing pressure has remained relatively constant over the past decades (ICCAT [2020](#)). Larval and fishery surveys indicate that, although larval abundances of ALB in western Mediterranean have dropped in recent years, adults target the same spawning sites and spawn during the same period (Saber et al. [2015](#); Alvarez-Berastegui et al. [2018](#)). Thus, it is unlikely that a change in their spawning grounds or in the spawning window is causing the drop in larval abundance. One intriguing possibility is that the increasing BFT population affects ALB abundance through predation on the larval stages.

Here, we model the predatory potential of larval BFT and assess its effect on early survival of ALB in the western Mediterranean Sea. Quantifying predator–prey encounters is difficult in any natural system, and for plankton we need to combine observations and mechanistic models (Kiørboe [2008](#)). We develop a size-dependent model of predation for BFT larvae to assess how their increasing density affect survival of ALB, including observed size distributions from surveys in a major spawning ground. Then, we compare ALB's predicted probability of survival and observed densities before (2001–2005) and after (2012–2017) the eastern stock recovery of BFT.

Material and methods

Field sampling and laboratory processing

We collected larval tuna with bongo nets in a major spawning ground around the Balearic Islands, western Mediterranean, in 11 surveys grouped in two discrete intervals from 2001 to 2005 and 2012 to 2017, representing periods before and after the BFT stock recovery, respectively (Supporting Information). Sampling was timed to coincide with the peak spawning of BFT, and all 1429 samples were preserved in 4% formalin buffered with borax.

In the laboratory, we counted and identified all fishes to the lowest possible taxon and measured standard length (SL) for ALB and BFT with a camera-attached stereoscope and Image-Pro analysis software. Larval lengths were then corrected for the effect of shrinkage in formalin so we can use functional parameters obtained from live experiments (Supporting Information).

Defining predators and prey

BFT (and ALB) larvae complete the notochordal flexion (bending of the notochord in the caudal fin) and switch to a dominantly piscivorous diet at about 7.5 mm SL (Blanco et al. [2019](#); Uriarte et al. [2019](#)). Therefore, we assume all BFT larvae ≥ 7.5 mm to be piscivorous predators on ALB that have not yet completed the notochordal flexion (Fig. [1](#)). Yolk-sac is the smallest and least developed of the larval stages, with a negligible ability to detect and escape attacks from piscivorous larvae. We used the lower standard deviation of pre-flexion larval size (4.2 mm; Fig. S1) as the threshold of first feeding and, since larvae ≤ 4.1 mm are yolk-sack larvae, their probability of capture success $p = 1$. Larvae between 4.2 and 7.4 mm SL gradually flex their notochord and improve their swimming and evasive abilities (Reglero et al. [2015](#); Blanco et al. [2019](#); Downie et al. [2020](#)). For these, we assume that the probability of capture success p_{ij} for a BFT of size i hunting an ALB of size j decreases with relative predator–prey length (Eq. [1](#)):

$$p_{ij} = \begin{cases} 1 \text{ for } L_j \leq 4.1 \\ \left(1 - \frac{L_j - 4.1}{L_i - 4.1}\right)^k \text{ for } L_j > 4.1 \end{cases} \quad (1)$$
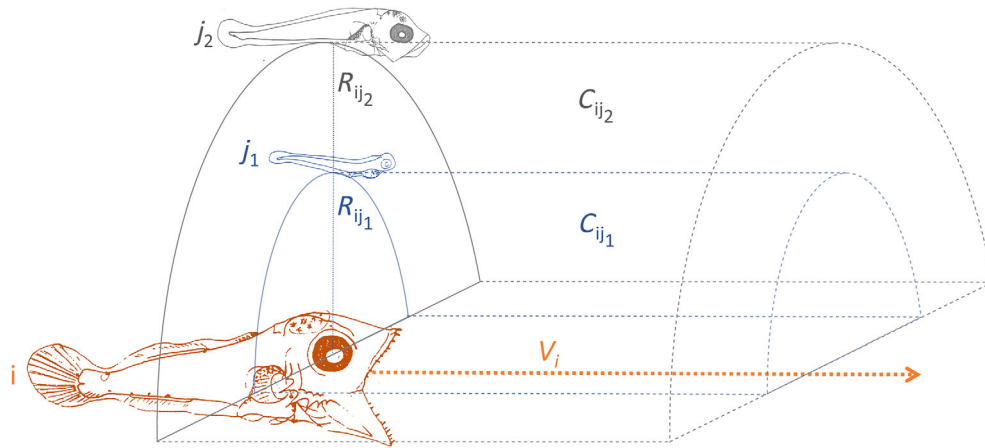
Fig. 1. Schematic representation of the modeled visual radius R_{ij} (m) and clearance rate C_{ij} (m³ s⁻¹) for each predator–prey interaction between BFT larvae (i = 7.5–13 mm) cruising at a speed V_i of 3 body lengths (L_i) s⁻¹ and albacore larvae ($j \leq 7.4$ mm).

Here, k is set to a basic value of 10 (*see* Supporting Information for justification and sensitivity analysis of k) and L_i and L_j are the BFT and ALB SL (m), respectively.

The predator–prey encounter model

BFT larvae are visual predators that detect prey at increasing distance through ontogeny (Hilder et al. 2019). Here, we quantify how often a BFT larva encounters and captures an ALB larva based on a mechanistic model for volume scanned for prey and survey data on densities and size distributions of both larval species. From this, we integrate the potential predation mortality suffered by ALB larvae.

First, we need to know how far away a BFT larva can detect an ALB, and how this depends on the body size or ontogeny of both predator and prey. The ability to resolve and detect objects depend, among other things, on the eye size, focal length and density of rods, and cones on the retina—the visual acuity (Caves et al. 2018; Hilder et al. 2019). Visual acuity can be measured as minimum separable angle M, which determines the smallest visual angle at which two separate objects can be distinguished. Here, we use an empirical estimate of M from the southern BFT *Thunnus macoyii*: $M = 4.699L^{-1.129}$ where L is the prey length (Hilder et al. 2019). Southern BFT is a close relative of Atlantic BFT with a similar ontogenetic development of eye and retina (Yúfera et al. 2014). The maximum visual prey detection distance R_{ij} (m) of a BFT of length i on an ALB of length j then becomes

$$R_{ij} = \frac{0.5L_j z q}{\tan(0.5M_i)} \qquad (2)$$

where $z = 0.5$ is the behavioral/anatomical correction ratio (Job and Bellwood 1996). This equation applies to a spherical object; therefore, we reduce R_{ij} by $q = 0.5$ since the projected image area of a fish larva is about half that of a circle.

Southern BFT larvae develop higher cone density in the ventral retinal region, which suggest they detect most prey looking upward with the surface as a contrasting background (Hilder et al. 2019). We therefore reduce their potential sectional search area from a full circle to a half circle (Fig. 1) (Fiksen and Folkvord 1999). We further assume random directional swimming of prey and predators in three dimensions, and apply the encounter model of Gerritsen and Strickler (1977) to calculate the clearance rate C_{ij} (m³ h⁻¹), or volume of water scanned by a BFT of size i for ALB of size j per hour:

$$C_{ij} = 0.5\pi R_{ij}^2 \frac{V_j^2 + 3V_i^2}{3V_i} \qquad (3)$$

where V_i and V_j are the BFT and ALB swimming velocities (m h⁻¹), respectively. Larval BFT swimming velocity V_i is about 3 body-lengths s⁻¹ (Reglero et al. 2015), and we assume V_j is the same. The rate E_{ij} at which an ALB of size j may encounter BFT of size i per hour is obtained by simply multiplying C_{ij} by the predator density D_i (BFT larvae m⁻³), $E_{ij} = C_{ij} \times D_i$. We assessed the sensitivity of visual radius (m) and clearance rate (m³ h⁻¹) to all model parameters and predictions (Supporting Information).

For each ij predator–prey size combination (Fig. 1), a BFT larva's immediate consumption rate is $E_{ij} \times P_{ij}$. BFT larvae do not feed in darkness (Blanco et al. 2017), and we assume no satiation or handling limitations, which is reasonable given the low observed densities of ALB (Fig. S6). Therefore, the daily consumption rate becomes $E_{ij} \times P_{ij} \times h$ and daily survival chance is $S_{ij} = \exp^{-E_{ij} \times P_{ij} \times h}$, where h is the number of daylight hours (15 h). Following the multiplication rule of probability, for each station, all S_{ij} of a given j-size ALB can be multiplied to calculate daily chance S_j to survive to all size-predators i combined. Then, we multiply $S_j \times D_j$ to find

the density of surviving ALB after 1 d of exposure to predation.

Size-structure and vulnerability to increasing BFT abundance

For ALB, survival depends on BFT's total density ΣD_i and relative size. Field densities of piscivorous BFT range from 0 to 0.168 larvae m^{-3}, and the size-structure of ALB and BFT is unique in each station. Because we want to test the vulnerability of each ALB cohort based on its size structure, regardless of the predator size-structure, we standardize BFT to an idealized continuous size structure (Supporting Information) and estimate ALB survival of each station to increasing densities of BFT. To further illustrate how piscivory differs among ALB size-classes, we simulate another idealized size-structured cohort, this time of larval ALB, and focus on size-class effects at $\Sigma D_i = 0.002$, 0.020, 0.080, and 0.168 BFT larvae m^{-3}.

BFT and survival of ALB larvae

We test the effect of BFT on ALB survival along spatial and temporal dimensions. Spatially, we use annual survey data to map piscivorous BFT distribution over the spawning ground, including their size-structure, and estimate daily probability of

dying (1 – probability of survival) for a vulnerable (4.1 mm SL) ALB yolk-sack larva at each station. Mortality will be greater in stations with denser and larger BFT than in stations with fewer and smaller BFT and will have no effect where BFT are absent (89.8% of surveyed stations).

For the temporal analysis, we apply a Welch's two-sample *t*-test to compare densities and daily probability of survival for a 4.1-mm ALB yolk-sack larva in each sampling station before and after the BFT recovery. Then, we correlate the temporal trends in ALB larval densities in relation with presence and abundance of piscivorous BFT and in relation to their predatory potential (survival for a 4.1-mm yolk-sack larva).

Results

Size-structure and vulnerability to increasing BFT abundance

Piscivorous BFT (≥ 7.5 mm SL) accounted for less than 1% of the total BFT larvae observed in the field, but they were relatively widespread (in 10.2% of all stations) and found in densities up to 0.167 larvae m^{-3}. Almost half the stations with
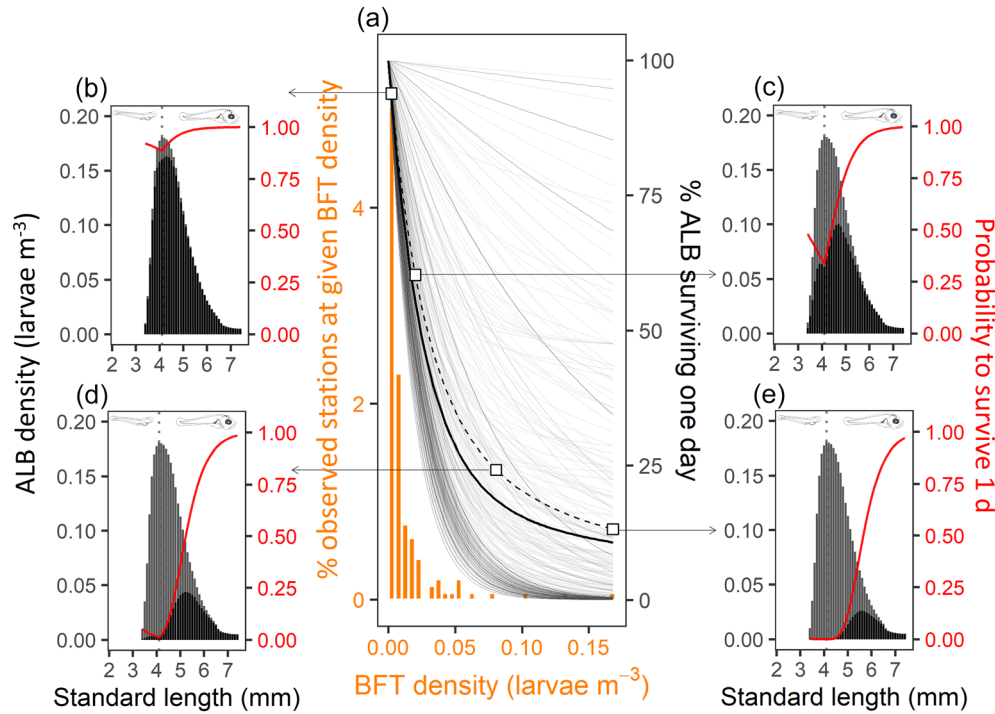

Fig. 2. Daily survival probability of ALB larvae exposed to increasing densities of BFT (≥ 7.5 mm SL). (**a**) Orange bars indicate frequency of observed field stations with specific BFT densities (larvae m^{-3}) excluding zeros (89.8%); gray lines indicate daily proportion of surviving ALB to increasing BFT density (ΣD_i) given the ALB size structure of each sampled station ($n = 1429$ stations), solid black line is the mean of all stations, and the dashed black line represents a simulated idealized size-structure (corresponding to the gray bars in panels (**b–e**); white squares set at density $\Sigma D_i = 0.002$, 0.020, 0.080 and 0.168 BFT larvae m^{-3}. (**b–e**) Size distributions of a simulated idealized cohort of ALB before (gray bars in the background) and after (black bars) 1 d of exposure to four BFT densities $\Sigma D_i = 0.002$ (**b**), 0.020 (**c**), 0.080 (**d**), and 0.168 (**e**) larvae m^{-3}. The proportion of ALB removed in each case is 6%, 40%, 76%, and 87%, respectively. Red line indicates daily probability of surviving of ALB in each size group. The vertical dotted line is the size-limit of yolk-sack larvae (≤ 4.1 mm).
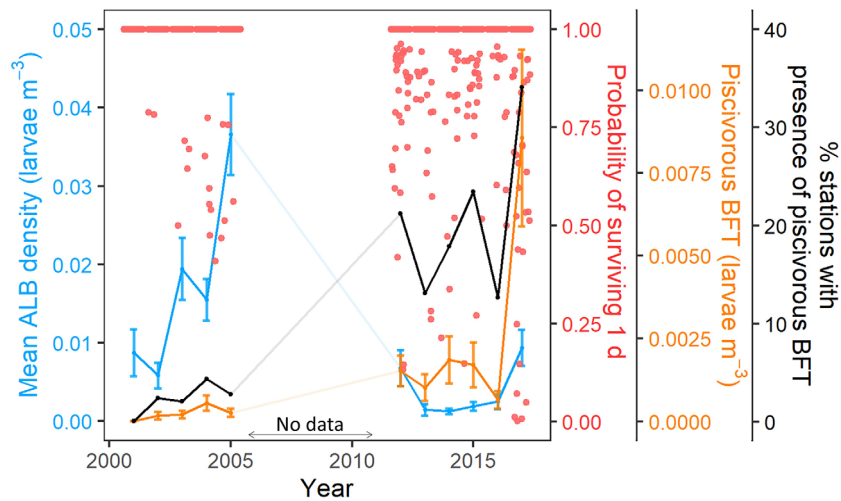
Fig. 3. Temporal trends on abundances and predatory pressure of bluefin tuna (BFT) and albacore (ALB). Annual mean observed ALB density (blue; mean larvae m^{-3} ± SE), abundance of BFT (orange; mean larvae m^{-3} ± SE), percent stations with presence of piscivorous larvae (black); and probability that a vulnerable yolk-sac ALB larva (4.1 mm SL) survive 1 d in the field considering the density and size-structure of BFT found in each station (red dots).

piscivorous BFT had < 0.005 larvae m^{-3}, and only three stations (0.2%) had more than 0.10 larvae m^{-3} (Fig. 2a).

The average proportion of observed ALB that would survive daily predation at the highest density of BFT is 17.2% (0.168 larvae m^{-3}, assuming idealized BFT size structure; Fig. S5) (Fig. 2a). However, observed ALB size structures differ among stations, resulting in large variation in survival. Among the 33.3% stations with the presence of ALB (Fig. S6), 81% of them had only small (< 4.5 mm) ALB. Thus, ALB larvae at most stations are vulnerable to high BFT abundance (Fig. 2a).

BFTs' killing potential increase proportionally with density, but mostly small ALB larvae are vulnerable to predation. In the simulated size-structured cohort of larval ALB (Fig. 2b–e), their probability to survive 1 d increases with size after the yolk-sack larvae threshold, regardless of predator abundance. Small individuals (< 4.5 mm SL) are removed much faster than larger individuals (4.5–7.4 mm), which is illustrated with a greater drop of surviving ALB. Thus, although BFT's killing potential increases proportionally with density, the size-distribution of the surviving ALB cohort will differ depending on BFT density.

BFT and survival of ALB larvae

Overall, the probability that an ALB is predated by a piscivorous BFT larva is low and patchy due to the absence of piscivorous BFT in most stations. However, patches of high daily mortality were up to 5 times larger and over 10 times more abundant in the 2012–2017 interval compared to the 2001–2005 interval (Fig. S7). Estimated daily mortality was lowest in 2001 when no piscivorous BFT was observed and greatest off southeast Ibiza in 2017, where vulnerable ALB (i.e., 4.1 mm SL yolk-sack larva) had < 1% estimated daily chance to survive predation from BFT in an area of 1000 km^2.

Across the 17-yr period of this study, BFTs' presence and abundance increased after the stock recovery (Fig. 3). Thus, ALB's estimated daily probability of survival dropped in 2012–2017 compared to 2001–2005 (*F*-test, $p < 0.001$). Conversely, ALB was less abundant in 2012–2017 than in 2001–2005 despite interannual fluctuations within each period (*F*-test, $p < 0.001$).

Discussion

Trophic interactions among fish larvae have been largely neglected, but we show that some voracious and piscivorous larvae can be an important driver of mortality in other fish species. Piscivorous bluefin tuna (BFT) larvae can cause severe mortality in small ALB larvae and truncate their size distribution. Even at low densities (0.02 larvae m^{-3}), BFT can kill more than half the yolk-sack and small pre-flexion ALB larvae in a single day (Fig. 2c), and real predation may exceed the values reported here because piscivorous BFT are likely underestimated due to net avoidance (Habtes et al. 2014). This predator–prey interaction is strong because larval BFT are unusually abundant in the western Mediterranean spawning grounds compared to tunas elsewhere (Ohshimo et al. 2017; Tawa et al. 2020). However, larvae of other billfishes and scombrids may have an even greater piscivorous potential than BFT, as some are more voracious (Llopiz and Hobday 2015) and can be more abundant. Thus, strong piscivorous interactions among fish larvae are likely more widespread than previously thought. This conclusion may extend to freshwater systems too, as fishes like pike *Esox* spp. or pikeperch *Sander* spp. also become piscivorous during their larval stage (Colchen et al. 2020).

Our model shows that the increase in piscivorous BFT larvae has resulted in an increased risk of mortality for ALB, but does this mean that BFT can reduce the recruitment potential of ALB? Predation only takes place when both predator and prey co-occur, and because only a fraction of newly hatched individuals survive to the post-flexion stage, BFT are relatively few and patchy by the time they become piscivorous. Thus, most areas of the ALB spawning ground are relatively safe from piscivorous BFT (Fig. S7). However, the number and size of these patches has increased after the BFT stock recovery, reducing the ALB piscivore-safe zones. Piscivorous BFT rose from an average 0.0003 to 0.0016 larvae m^{-3} after the stock recovery and estimated mean daily survival of ALB dropped from 99% to 95% (Fig. 3). This suggests that predator–prey interactions may have contributed to the reduction of observed ALB density with the recovery of BFT (Fig. 3). Nonetheless, the increase in BFT piscivorous pressure is just one of several contributing processes driving the ALB decay, as the larval abundances of both species are not always negatively correlated. In 2017, for instance, larval abundances of both species increased, suggesting that factors like warm water temperature, food availability, or low abundance of invertebrate predators (Fiksen and Reglero 2021; Ottmann et al. 2021) could favor both species.

Other processes, like a decrease of ALB biomass due to fishing activities (ICCAT 2021), changes in food availability (Gleiber et al. 2020), or increase of tropical species with piscivorous behavior (Báez et al. 2018) may also contribute to the observed decline of ALB larval densities, especially in the stations where piscivorous BFT is absent. It is difficult to say which processes have a greater contribution to ALB mortality, as they may vary over time and space. The effect of piscivorous BFT, for instance, is strongest at the beginning of ALB's spawning season, as this is when BFT is most actively reproducing (Reglero et al. 2018b). Mesocosm experiments under different temperature and food regimes can help determine the vulnerability of ALB larvae to other habitat conditions.

A meta-analysis study (Mittelbach and Persson 1998) reveals that freshwater fishes that develop piscivorous behavior early in life tend to be larger at hatch, grow faster, and spawn earlier than their prey. In our case, both tuna species have similar size-at-hatch and growth rate; thus, it is the early spawning of BFT (Reglero et al. 2018b) that results in a priority effect. The fact that their larvae are large enough to be piscivorous when ALB yolk-sack and pre-flexion larvae are most abundant may be an adaptive life-history strategy in a long-distance migrator to provide fish prey to their offspring and simultaneously reduce food competition with other larvae of the same guild (Siepielski et al. 2020), yet this hypothesis remains untested. Either way, it suggests that the timing of spawning is an important modulator of the interaction strength among piscivorous fishes of the same guild.

Predation and predator-related processes are the major drivers of fish mortality, especially during the early stages of life (Bailey and Houde 1989; Houde 2008; Fouzai et al. 2019). However, mortality processes in larval stages may differ from those in the juvenile stage. Current studies show that juvenile ALB have not been observed in stomach content of other juvenile or adult scombrids (Fletcher et al. 2013; Sorell et al. 2017; Varela et al. 2019), and juvenile ALB are thought to be too few to cause density-dependent regulation (Arregui et al. 2006; Bakun 2013). Thus, although predation and density-dependence may occur in juvenile stages, it appears that processes driving mortality of larval stages have a heavier leverage on recruitment success (Watai et al. 2017; Ishihara et al. 2019).

The eastern stock of Atlantic BFT has recovered from overfishing thanks to effective fisheries management (Porch et al. 2019), but the rise of BFT may have unintended consequences on the Mediterranean ALB stock due to predation in larval stages. Predator–prey interactions can cause alternative stable states in both marine and freshwater systems (Barkai and McQuaid 1988; Persson et al. 2007; Eklöf et al. 2020), where changes in the prey or predator populations, often triggered by human activities, can reverse the predator–prey role. Although the degree to which larval piscivory can affect recruitment of ALB remains uncertain, this study is the first to consider population-level effects of a fish by a larval predator of the same guild. Clarifying the effect that the recovery of BFT may have on ALB is important to understand the population dynamics of both species. While the stock appears to be declining, current management of the Mediterranean ALB fishery aims to "avoid increases in catch and effort" (Alvarez-Berastegui et al. 2018; ICCAT 2021). Now that some stocks of top predator fishes are recovering world-wide (Hilborn et al. 2020), further understanding of trophic interactions between commercially important species can help decision makers move beyond single-stock management.

References

Alemany, F., and others. 2010. Characterization of the spawning habitat of Atlantic bluefin tuna and related species in the Balearic Sea (western Mediterranean). Prog. Oceanogr. **86**: 21–38. doi:10.1016/j.pocean.2010.04.014

Alvarez-Berastegui, D., and others. 2018. Integrating reproductive ecology, early life dynamics and mesoscale oceanography to improve albacore tuna assessment in the Western Mediterranean. Fish. Res. **208**: 329–338. doi:10.1016/j.fishres.2018.08.014

Arregui, I., H. Arrizabalaga, D. S. Kirby, and J. M. Martin-Gonzalez. 2006. Stock–environment–recruitment models for North Atlantic albacore (*Thunnus alalunga*). Fish. Oceanogr. **15**: 402–412. doi:10.1111/j.1365-2419.2005.00399.x

Báez, J. C., P. Pascual-Alayón, M. L. Ramos, and F. J. Abascal. 2018. Túnidos tropicales: Calentamiento global y seguridad

alimentaria, una visión global. Rev. Biol. Mar. Oceanogr. **53**: 1–8. doi:10.4067/S0718-19572018000100001

Bailey, K. M., and E. D. Houde. 1989. Predation on eggs and larvae of marine fishes and the recruitment problem, p. 1–83. *In Advances in marine biology*. Elsevier. doi:10.1016/S0065-2881(08)60187-X

Bakun, A. 2013. Ocean eddies, predator pits and bluefin tuna: Implications of an inferred 'low risk-limited payoff' reproductive scheme of a (former) archetypical top predator. Fish Fish. **14**: 424–438. doi:10.1111/faf.12002

Barkai, A., and C. McQuaid. 1988. Predator-prey role reversal in a marine benthic ecosystem. Science **242**: 62–64. doi:10.1126/science.242.4875.62

Blanco, E., P. Reglero, A. Hernández de Rojas, A. Ortega, F. de la Gándara, and A. Folkvord. 2019. The effect of nutritional condition by two nucleic acid derived indices on the growth to post-flexion of Atlantic bluefin tuna and Atlantic bonito larvae. J. Exp. Mar. Biol. Ecol. **519**: 151182. doi:10.1016/j.jembe.2019.151182

Blanco, E., P. Reglero, A. Ortega, F. de la Gándara, Ø. Fiksen, and A. Folkvord. 2017. The effects of light, darkness and intermittent feeding on the growth and survival of reared Atlantic bonito and Atlantic bluefin tuna larvae. Aquaculture **479**: 233–239. doi:10.1016/j.aquaculture.2017.05.020

Caves, E. M., N. C. Brandley, and S. Johnsen. 2018. Visual acuity and the evolution of signals. Trends Ecol. Evol. **33**: 358–372. doi:10.1016/j.tree.2018.03.001

Colchen, T., A. Dias, E. Gisbert, F. Teletchea, P. Fontaine, and A. Pasquet. 2020. The onset of piscivory in a freshwater fish species: Analysis of behavioural and physiological traits. J. Fish Biol. **96**: 1463–1474. doi:10.1111/jfb.14322

Downie, A. T., B. Illing, A. M. Faria, and J. L. Rummer. 2020. Swimming performance of marine fish larvae: Review of a universal trait under ecological and environmental pressure. Rev. Fish Biol. Fish. **30**: 93–108. doi:10.1007/s11160-019-09592-w

Eklöf, J. S., G. Sundblad, M. Erlandsson, S. Donadi, J. P. Hansen, B. K. Eriksson, and U. Bergström. 2020. A spatial regime shift from predator to prey dominance in a large coastal ecosystem. Commun. Biol. **3**: 459. doi:10.1038/s42003-020-01180-0

Fiksen, Ø., and A. Folkvord. 1999. Modelling growth and ingestion processes in herring *Clupea harengus* larvae. Mar. Ecol. Prog. Ser. **184**: 273–289. doi:10.3354/meps184273

Fiksen, Ø., and P. Reglero. 2021. Atlantic bluefin tuna spawn early to avoid metabolic meltdown in larvae. Ecology **103** (1):1–8. doi:10.1002/ecy.3568

Fletcher, N., I. E. Batjakas, and G. J. Pierce. 2013. Diet of the Atlantic bonito *Sarda sarda* (Bloch, 1793) in the Northeast Aegean Sea. J. Appl. Ichthyol. **29**: 1030–1035. doi:10.1111/jai.12164

Folkvord, A. 1997. Ontogeny of cannibalism in larval and juvenile fishes with special emphasis on Atlantic cod,

p. 251–278. *In* R. C. Chambers and E. A. Trippel [eds.], *Early life history and recruitment in fish populations*. Springer.

Fouzai, N., A. F. Opdal, C. Jørgensen, and Ø. Fiksen. 2019. Dying from the lesser of three evils: Facilitation and non-consumptive effects emerge in a model with multiple predators. Oikos **128**: 1307–1317. doi:10.1111/oik.05631

Gerritsen, J., and J. R. Strickler. 1977. Encounter probabilities and community structure in zooplankton: A mathematical model. J. Fish. Res. Bd. Can. **34**: 73–82. doi:10.1139/f77-008

Gleiber, M. R., S. Sponaugle, and R. K. Cowen. 2020. Some like it hot, hungry tunas do not! Implications of temperature and plankton food web dynamics on growth and diet of tropical tuna larvae. ICES J. Mar. Sci. **77**: 3058–3073. doi:10.1093/icesjms/fsaa201

Habtes, S., F. E. Muller-Karger, M. A. Roffer, J. T. Lamkin, and B. A. Muhling. 2014. A comparison of sampling methods for larvae of medium and large epipelagic fish species during spring SEAMAP ichthyoplankton surveys in the Gulf of Mexico: Gulf of Mexico larval fish sampling gear. Limnol. Oceanogr.: Methods **12**: 86–101. doi:10.4319/lom.2014.12.86

Hilborn, R., and others. 2020. Effective fisheries management instrumental in improving fish stock status. Proc. Natl. Acad. Sci. USA **117**: 2218–2224. doi:10.1073/pnas.1909726116

Hilder, P. E., S. C. Battaglene, N. S. Hart, S. P. Collin, and J. M. Cobcroft. 2019. Retinal adaptations of southern bluefin tuna larvae: Implications for culture. Aquaculture **507**: 222–232. doi:10.1016/j.aquaculture.2019.04.024

Houde, E. D. 2008. Emerging from Hjort's shadow. J. Northwest Atl. Fish. Sci. **41**: 53–70. doi:10.2960/J.v41.m634

ICCAT. 2020. 2020 SCRS advice to the Comission. ICCAT **17**: 1–362.

ICCAT. 2021. Report of the intersessional meeting of the albacore species group including the Mediterranean albacore stock assessment. SCRS SCRS/2021/009, Collect. Vol. Sci. Pap. ICCAT **78**: 1–36.

Ishihara, T., M. Watai, S. Ohshimo, and O. Abe. 2019. Differences in larval growth of Pacific bluefin tuna (*Thunnus orientalis*) between two spawning areas, and an evaluation of the growth-dependent mortality hypothesis. Environ. Biol. Fishes **102**: 581–594. doi:10.1007/s10641-019-00855-w

Job, S. D., and D. R. Bellwood. 1996. Visual acuity and feeding in larval *Premnas biaculeatus*. J. Fish Biol. **48**: 952–963. doi:10.1111/j.1095-8649.1996.tb01489.x

Kaji, T., J. Shoji, M. Aoyama, and M. Tanaka. 2002. Highly specialized development of the digestive system in piscivorous scombrid larvae. Fish. Res. **68**: 884–887. doi:10.2331/fishsci.68.sup1_884

Kiørboe, T. 2008, *A mechanistic approach to plankton ecology*. Princeton Univ. Press.

Llopiz, J. K., and A. J. Hobday. 2015. A global comparative analysis of the feeding dynamics and environmental conditions of larval tunas, mackerels, and billfishes. Deep-Sea Res. Part II: Top. Stud. Oceanogr. **113**: 113–124. doi:10.1016/j.dsr2.2014.05.014

Mittelbach, G. G., and L. Persson. 1998. The ontogeny of piscivory and its ecological consequences. Can. J. Fish. Aquat. Sci. **55**: 12. doi:10.1139/f98-041

Ohshimo, S., and others. 2017. Horizontal distribution and habitat of Pacific bluefin tuna, *Thunnus orientalis*, larvae in the waters around Japan. Bull. Mar. Sci. **93**: 769–787. doi:10.5343/bms.2016.1094

Ottmann, D., Ø. Fiksen, M. Martín, F. Alemany, and L. Prieto. 2021. Spawning site distribution of a bluefin tuna reduces jellyfish predation on early life stages. Limnol. Oceanogr. **66**: 3669–3681. doi:10.1002/lno.11908

Persson, L., P.-A. Amundsen, A. M. De Roos, A. Klemetsen, R. Knudsen, and R. Primicerio. 2007. Culling prey promotes predator recovery—alternative states in a whole-Lake experiment. Science **316**: 1743–1746. doi:10.1126/science.1141412

Porch, C. E., S. Bonhommeau, G. A. Diaz, H. Arrizabalaga, and G. Melvin. 2019. The journey from overfishing to sustainability for Atlantic bluefin yuna, *Thunnus thynnus*, p. 3–44. *In The future of bluefin tunas: Ecology, fisheries management, and conservation*. Johns Hopkins Univ. Press.

Reglero, P., and others. 2018*a*. Vertical distribution of Atlantic bluefin tuna *Thunnus thynnus* and bonito *Sarda sarda* larvae is related to temperature preference. Mar. Ecol. Prog. Ser. **594**: 231–243. doi:10.3354/meps12516

Reglero, P., and others. 2018*b*. Atlantic bluefin tuna spawn at suboptimal temperatures for their offspring. Proc. R. Soc. B **285**: 20171405. doi:10.1098/rspb.2017.1405

Reglero, P., D. Tittensor, D. Álvarez-Berastegui, A. Aparicio-González, and B. Worm. 2014. Worldwide distributions of tuna larvae: Revisiting hypotheses on environmental requirements for spawning habitats. Mar. Ecol. Prog. Ser. **501**: 207–224. doi:10.3354/meps10666

Reglero, P., N. Zaragoza, E. Blanco, F. de la Gandara, A. P. Torres, and A. Ortega. 2015. Routine swimming speed of bluefin tuna larvae measured in the laboratory. Proceedings of the 39th Annual Larval Fish Conference.

Saber, S., J. Ortiz de Urbina, M. J. Gómez-Vives, and D. Macías. 2015. Some aspects of the reproductive biology of albacore *Thunnus alalunga* from the western Mediterranean Sea. J. Mar. Biol. Assoc. **95**: 1705–1715. doi:10.1017/S002531541500020X

Siepielski, A. M., A. Z. Hasik, T. Ping, M. Serrano, K. Strayhorn, and S. P. Tye. 2020. Predators weaken prey intraspecific competition through phenotypic selection I. Donohue [ed.]. Ecol. Lett. **23**: 951–961. doi:10.1111/ele.13491

Sorell, J. M., J. L. Varela, N. Goñi, D. Macías, H. Arrizabalaga, and A. Medina. 2017. Diet and consumption rate of Atlantic bluefin tuna (*Thunnus thynnus*) in the Strait of Gibraltar. Fish. Res. **188**: 112–120. doi:10.1016/j.fishres.2016.12.012

Tawa, A., T. Kodama, K. Sakuma, T. Ishihara, and S. Ohshimo. 2020. Fine-scale horizontal distributions of multiple species of larval tuna off the Nansei Islands, Japan. Mar. Ecol. Prog. Ser. **636**: 123–137. doi:10.3354/meps13216

Torres, A. P., P. Reglero, R. Balbin, A. Urtizberea, and F. Alemany. 2011. Coexistence of larvae of tuna species and other fish in the surface mixed layer in the NW Mediterranean. J. Plankton Res. **33**: 1793–1812. doi:10.1093/plankt/fbr078

Uriarte, A., and others. 2019. Evidence of density-dependent cannibalism in the diet of wild Atlantic bluefin tuna larvae (*Thunnus thynnus*) of the Balearic Sea (NW-Mediterranean). Fish. Res. **212**: 63–71. doi:10.1016/j.fishres.2018.12.013

Varela, J. L., J. P. Cañavate, A. Medina, and G. Mourente. 2019. Inter-regional variation in feeding patterns of skipjack tuna (*Katsuwonus pelamis*) inferred from stomach content, stable isotope and fatty acid analyses. Mar. Environ. Res. **152**: 104821. doi:10.1016/j.marenvres.2019.104821

Watai, M., T. Ishihara, O. Abe, S. Ohshimo, and C. A. Strussmann. 2017. Evaluation of growth-dependent survival during early stages of Pacific bluefin tuna using otolith microstructure analysis. Mar. Freshw. Res. **68**: 2008. doi:10.1071/MF16337

Yúfera, M., J. B. Ortiz-Delgado, T. Hoffman, I. Siguero, B. Urup, and C. Sarasquete. 2014. Organogenesis of digestive system, visual system and other structures in Atlantic bluefin tuna (*Thunnus thynnus*) larvae reared with copepods in mesocosm system. Aquaculture **426–427**: 126–137. doi:10.1016/j.aquaculture.2014.01.031